Title
THE AFTERPULSE TIME SPECTRA OF HIGH-SPEED PHOTON DETECTORS

Author
Leskovar, B.

Publication Date
1985

Lawrence Berkeley Laboratory
UNIVERSITY OF CALIFORNIA

Engineering Division

Presented at the Laser 85 OptoElectronics International Congress, Munich, West Germany, July 1-5, 1985; and to be published in the Proceedings

THE AFTERPULSE TIME SPECTRA OF HIGH-SPEED PHOTON DETECTORS

B. Leskovar

January 1985

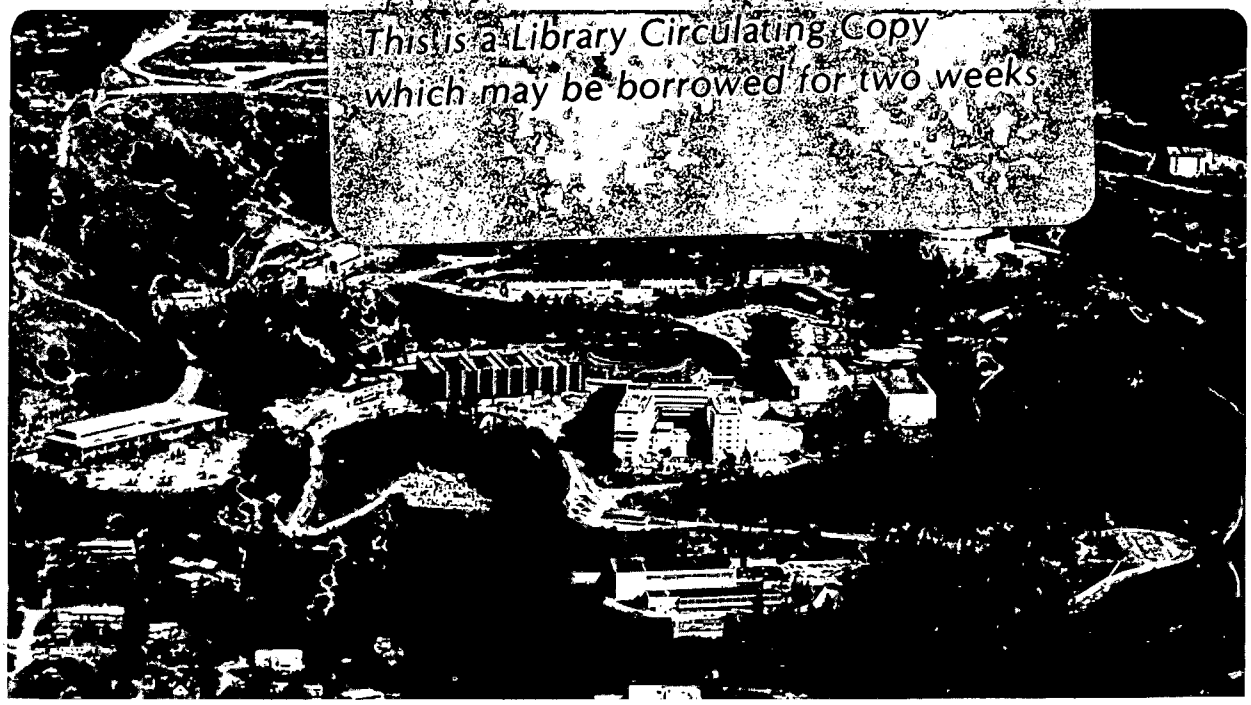

Prepared for the U.S. Department of Energy under Contract DE-AC03-76SF00098

DISCLAIMER

To Be Presented at the Laser 85
OptoElectronics International
Congress, Munich, West Germany,
July 1 - 5, 1985

LBL-18909

THE AFTERPULSE TIME SPECTRA OF HIGH-SPEED PHOTON DETECTORS

Branko Leskovar

Lawrence Berkeley Laboratory
University of California
Berkeley, California 94720 U.S.A.

January 10, 1985

Prepared for the U.S. Department of Energy
under Contract No. DE-AC03-76SF0098

THE AFTERPULSE TIME SPECTRA OF HIGH-SPEED PHOTON DETECTORS

Branko Leskovar
Lawrence Berkeley Laboratory
University of California
Berkeley, California 94720 U.S.A.

ABSTRACT

Recent progress of understanding of the afterpulse time spectra of high-speed photon detectors using photoemission and secondary emission processes is reviewed and summarized. Furthermore, the afterpulse time spectra of high-gain conventionally designed and microchannel plate photon detectors has been investigated. Specifically, the devices studied included RCA 8850, RCA 8854 and ITT F 4129f photomultipliers. Descriptions are given of the measuring techniques.

INTRODUCTION

The afterpulse time spectrum of high speed photon detectors has been the subject of intensive experimental and theoretical investigations. Over the years improvements in fabrication and activation techniques have significantly reduced afterpulses from most photomultipliers. However, for some applications afterpulses still may introduce serious error. For example, in photon counting systems for subnanosecond fluorescence lifetime measurements,[1-3] photomultiplier afterpulses can generate small amplitude late artifactual peaks in the sample fluorescence profile. Also, in particle physics measuring systems, which use large numbers of photomultipliers in a 3-dimensional array, a significant amount of afterpulsing could introduce serious error in measuring particle trajectories.[4-6] Similarly, in plasma diagnostic experiments,[7,8] afterpulses from fast photon detectors can seriously distort observed pulse waveshape.

In general, the afterpulses are mostly produced as a result of the ionization of residual gases, such as He^+, H_2^+, N_2^+ and CO^+, in the volume between the photocathode and the first dynode as well as between various dynodes of the electron multiplier. A simplified component arrangement of a high-gain photomultiplier is shown in Fig. 1. The positive ions formed are accelerated toward the photocathode by the focusing electric field. On impact these ions liberate secondary electrons which produce an afterpulse signal. The number of these electrons depends upon the momentum and species of the ions and the photocathode composition. These afterpulses generally occur from 20 ns to several microseconds after the main pulse. The time of occurrence of the afterpulses can be closely correlated with the mass-to-charge ratio of the residual gas inside the glass envelope.

The time interval between the main output pulse and afterpulse, which is approximately equal to the transit time of the positive ion to photocathode is nearly independent of its point of origin. Therefore, the photomultiplier is approx. acting as a time-of-flight mass spectrometer. The peaks in the time spectrum of the afterpulse time distribution, corresponding to a particular ion, generally show some fine structure. The positive ion transit time varies as $(M/Z)^{1/2}$ where M/Z is the mass-to-charge ratio. The mass-to-charge ratio for ions H^+, H_2^+, He^{2+}, He^+, N^+, N_2^+ and CO^+ is 1, 2, 2, 4, 14, 28 and 28, respectively. By neglecting the initial thermal velocity and the transit time of a photoelectron from the photocathode to the point of ionization, the following equation for the time-of-flight of the colliding ion can be obtained[10]

$$t_{ion} = 7.2\times10^{-5}(M/Z)^{1/2}\int_{s_o}^{0}[V(s_o)-V(s)]^{-1/2}ds \qquad (1)$$

where the integration of the electric potential function is over the path from s_o (ion formation point) to the photocathode. V(s) is the potential in volts and s is the distance in meters.

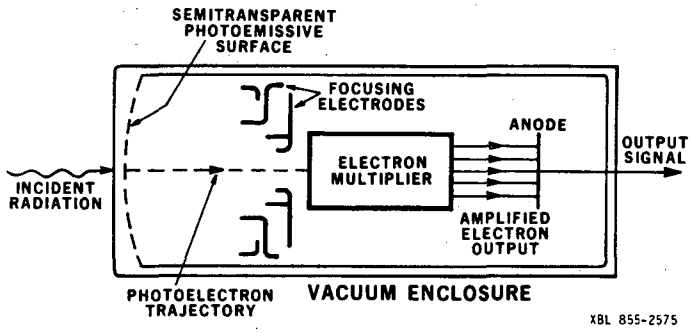

Fig. 1 Simplified component arrangement of a high-gain photomultiplier.

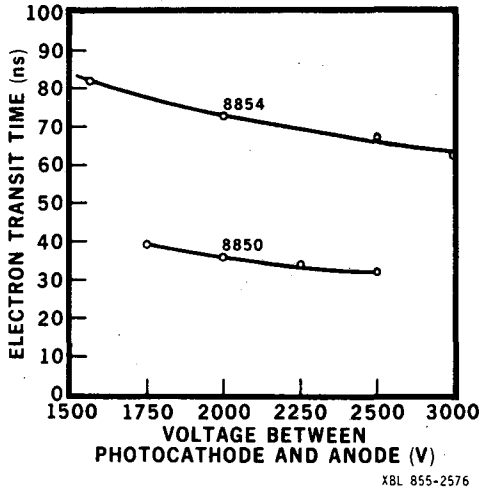

Fig. 2 Electron transit time as a function of the voltage between the photocathode and anode.

The afterpulse phenomena was studied systematically by several authors[9] who introduced trace amounts of various gasses into photomultipliers. Subsequently, in further works,[10-17] the physical origins of afterpulses were investigated, particularly with respect to the afterpulses which result from the diffusion of helium through the photomultiplier glass envelope.[18,19] Although the helium is present in small concentration in ambient air, it is sufficient so that its atoms, which can permeate readily through the glass envelope, can cause afterpulses. This effect may be enhanced often by the fact that photomultipliers are frequently used in lab-

oratories where ambient concentration of helium is significantly increased by emissions from helium Dewar bottles or from gas Cherenkov counters. Other phenomena may also cause afterpulsing, such as dynode fluorescence, electrical fields over the exposed glass of the envelope, etc. In order to measure this characteristic, a signal induced time spectrum must be taken of the anode output pulses.

In this paper, an effort has been made to investigate and review the afterpulse time spectra of some new generation commercially available photomultipliers in order to further our understanding of afterpulsing. Other characteristics of the photomultipliers, generally not available from manufacturers, have been measured and previously presented.[20-22] Specifically, time spectra have been studied of the new generation RCA 8850 and 8854 photomultipliers, which use conventional multiplier structures. Furthermore, the spectra have been investigated on a new generation of ITT 4129f extended life microchannel plate photomultipliers.

The RCA 8850 2" 12-stage photomultiplier is a modified version of the RCA 8575. Both have identical electron multiplier structures, electron optics and semitransparent cesium-potassium-antimony photocathodes deposited on a pyrex entrance window. The only significant difference between 8850 and 8575 is that 8850 has a cesium-activated gallium-phosphide secondary emitting surface on the first dynode. This surface has a secondary emission ratio of 30-50 instead of the 5-8 ratio of the conventional dynode material. The high pulse-height resolution of the 8850 makes it possible to set the threshold of the signal discriminator in the valley between the single and double photoelectron peaks, eliminating most of the single photoelectron pulses which are mostly thermionic initiated from the photocathode. The anode output pulse (10-90%) rise time is 2.4 ns at an applied voltage between the anode and cathode of 2500 V.

The RCA 8854 photomultiplier is a variant of the RCA 4522. It has a high gain GaP (Cs) first dynode followed by 13 BeO dynodes. The new RCA designation for the photocathode is 35 ET (formerly 118), which has a peak response at 400 nm and a quantum efficiency of 27%. Its spectral response extends from 200 nm to 600 nm. The maximum useful photocathode diameter is 114 mm; the anode output pulse (10-90%) rise time is approx. 3.2 ns at the supply voltage between the anode and cathode of 2500 V. This photomultiplier is designed for experimental research instrumentation where good pulse-height resolution and large photocathode areas are important.

The electron transit time as a function of voltage between the photocathode and anode was measured for both photomultipliers. The reference pulse was the electrical signal from a pulsed mercury light source. The transit time was measured from 50% of the leading-edge amplitude of the reference pulse to 50% of the leading-edge of the photomultiplier output pulse. The results are shown in Fig. 2; the electron transit time was 32 ns and 67 ns at 2500 V for 8850 and 8854, respectively.

The new ITT F 4129f photomultiplier has an S-20 photocathode with a maximum usable diameter of 18 mm and 3 microchannel plates in cascade for the electron multi-

plication. The plates are in a Z-configuration to reduce the positive ion feedback. The 3 plates are identical, having 12 μm diameter channels with length to diameter ratios of 40. Proximity focusing is used at the input and collector. The anode output pulse (10-90%) rise time is approx. 350 ps using microchannel plate voltage of 2500 V. In the ITT F 4129f device a protective film is provided between the photocathode and the microchannel plate which leads to a significant improvement in quantum efficiency stability and life expectancy.

DESCRIPTION OF THE MEASURING SYSTEM

The system described in Ref. 12 was used to measure afterpulse time spectra. A pulse generator was used to drive a light-emitting diode, type XP 21, which produced light pulses for the photomultiplier. The trigger pulse from the pulse generator was delayed and shaped and then used as a start pulse for the time-to-amplitude converter. The output pulse of the photomultiplier was used as the stop pulse for the converter after being processed by a constant fraction discriminator. In order to count the afterpulses which came immediately after the main photomultiplier pulse, the main output pulse was delayed after the start pulse. The time at which the main photomultiplier pulse occurred was taken as time zero. However, in order to count the afterpulses which occurred significantly later in time and with a very low count rate, the trigger pulse from the pulse generator was purposely delayed to come after the photomultiplier main pulse so that an output pulse from the converter would only occur when the photomultiplier generated an afterpulse. The output of the converter was then recorded and displayed on a pulse-height analyzer. In order to look for pulses many microseconds after the main pulse (the timing range of the converter being set accordingly) the operating frequency of the test system was quite low.

RESULTS AND DISCUSSIONS

The typical results of the measurements of afterpulse time spectra made on three RCA 8850 and 8854 photomultipliers are summarized in Table 1. Measurements were made using the voltage divider network suggested by RCA for fast pulse response. With 2500 V applied between the anode and cathode, the average gain was approx. 1.8×10^8, while the dark current was 4.6×10^{-8} A. With full photocathode illumination, under single photoelectron counting conditions at a rate of 100 kHz, afterpulses were detected in the typical time interval ranges of 18-22 ns and 342-415 ns, after the main output pulse for the RCA 8850.

When the light pulse intensity was increased so that pulses with three photoelectrons were produced by the 8850's, afterpulses were detected in the 19-22 ns and 342-413 ns time intervals, as before, in all three photomultipliers. Detailed re-

sults are given in Table 1. No afterpulse was observed beyond this range up to 68 μs under either the single or three photoelectron operating conditions. Afterpulses in the 342-415 ns range had a peak amplitude of approx. 2-3 times that of the main pulse. The photomultipliers tested were 10 years old. During this time they had been used mostly for calibration purposes of various single photon counting systems and high-gain photon detectors under control conditions in a standard laboratory environment.

Figure 3 shows the time distribution of output pulses on a logarithmic scale in the time interval 0-150 ns after the main photomultiplier pulse under 100 kHz single photoelectron counting rate. The first distribution at the beginning of the spectrum is the main output pulse of the photomultiplier. The second distribution represents the afterpulses which occurred 18 ns after the main pulse.

Figure 4 shows the same afterpulse spectrum on a linear time scale over the range 60-680 ns under 100 kHz single photoelectron counting rate. Afterpulses were also present from 342-415 ns after the main photomultiplier output pulse.

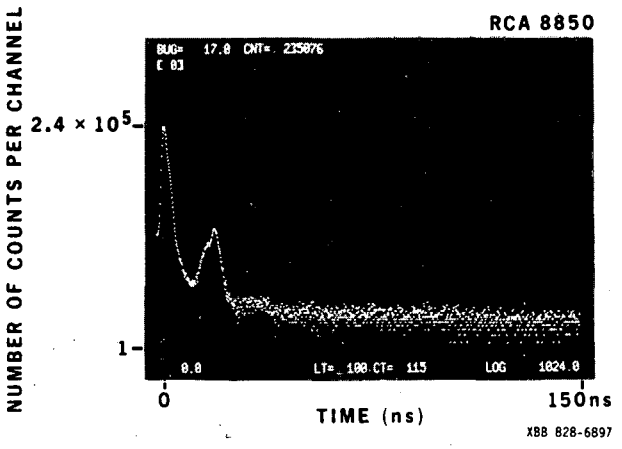

Fig.3 Time spectrum of anode output pulse between 0-150 ns for RCA 8850 with full photocathode illumination.

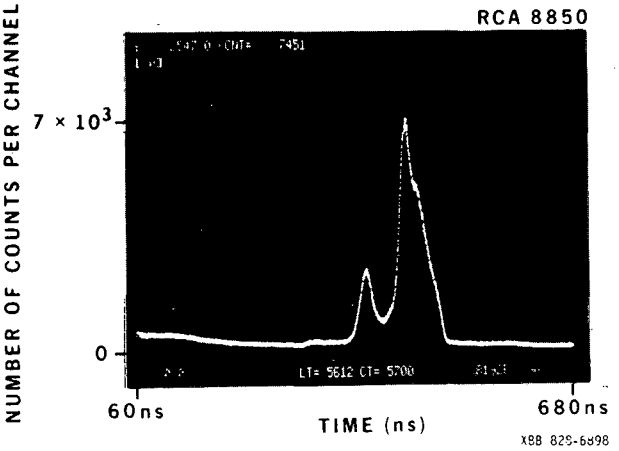

Fig. 4 Time spectrum of anode output pulse between 60-680 ns for RCA 8850 with full photocathode illumination.

The two groups of afterpulses occurring in the 342-415 ns range were attributed to He^+ ions which are created in the space between the photocathode and the first dynode and the second and third dynode. This conclusion is based on the time-of-flight of the helium ion from its point of origin to the photocathode and the ion mass-to-charge ratio. The two peak structure is clearly seen. The first peak of this distribution is caused by afterpulses generated by He^+ ions from the photocathode-first dynode region. The second peak of the distribution was studied by increasing the potential of each dynode by approx. 20 V. The effect of the voltage increase on afterpulse time distribution was observed. The time distribution was particularly sensitive to variations in the potential of the third dynode. This further substantiated the conclusion that the second peak is produced by afterpul-

ses generated by ions which are formed between the second and third dynode. This conclusion is in agreement with the results of afterpulse measurements obtained by Coates[7] for 8852 photomultiplier. However, no report has been made in literature on afterpulses which occurred in the 18-22 ns range after the main signal pulse. These pulses appeared at a lower rate but were consistently present in all three 8850's. Furthermore, the amplitude of these afterpulses was approx. 1/2 of the single photoelectron pulse amplitude, unlike those at the 342-415 ns time range which were 3 to 4 times larger.

The afterpulses in the 18-22 ns range were the most probably generated by He^+ ions, produced between the first and second dynode, striking the first dynode and causing the secondary emission. This conclusion is based on the calculation of electron transit time between the photocathode and the first dynode and the photomultiplier anode. Also the electric field distribution was taken into account. The 18-22 ns time range increased when the voltage between the photocathode and the first dynode/focusing electrode was decreased because of the change in the electric field intensity and distribution.

Afterpulse time spectra measurements were made on RCA 8854 photomultiplier using the voltage divider network described in Ref. 12. With 2500 V applied between anode and cathode, the gain was 3.5×10^8, while the dark current was 1.3×10^{-7} A. These photomultipliers were new when tested.

Under single photoelectron counting at a rate of 100 kHz, afterpulses were detected in the typical time interval ranges of 52-58.5 ns and 190-198 ns, after the main output pulse in all three 8854's. In the 450 ns-68 μs time range, afterpulses were detected in two out of three 8854's. In one photomultiplier at a 10 kHz pulse rate, 0.8 afterpulses/s were observed at 933 ns and the other at 1 kHz pulse rate gave 3.4 afterpulses/s at 12.5 μs. When the light pulse intensity was increased so that pulses with three photoelectrons were produced by the 8854's, afterpulses were detected in four time intervals in all three photomultipliers: 54.5-59 ns, 197-198 ns, 956-987 ns and 10.6-12.8 μs. Typical results are given in Table 1.

Figure 5 shows the time distribution of output pulses in the time interval 0-150 ns after the main photomultiplier pulse under a 100 kHz single photoelectron counting rate. The first distribution at the beginning of the spectrum is the main output pulse of the photomultiplier. The second distribution represents the afterpulses which occurred in the 52-58.5 ns time interval after the main pulse.

Figure 6 shows the afterpulse spectrum in the time interval 4.5-68 μs under 10 kHz-three photoelectron counting rate (limited by the time-to-amplitude converter timing range setting). Afterpulses were present in all three photomultipliers at 8.5 μs, 9.2 μs 12.8 μs and 14 μs after the main photomultiplier output pulse.

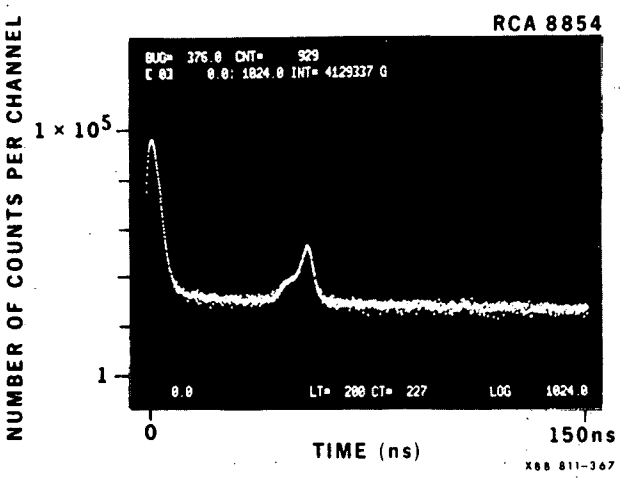

Fig. 5 Time spectrum of anode output pulse between 0-150 ns for RCA 8854 with full photocathode illumination.

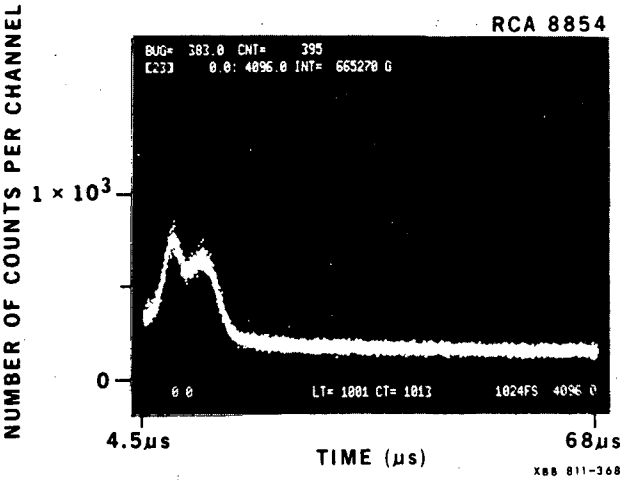

Fig. 6 Time spectrum of anode output pulse between 4.5-68 μs for RCA 8854 with full photocathode illumination.

Based on considerations similar to those given above, afterpulses in the 956-987 ns range were attributed to He^+ ions which are created in the space between the photocathode and the first dynode. This conclusion is in agreement with the results of afterpulse measurement obtained by Bartlett et al[19] for a similarly designed photomultiplier 4522. However, no report has been made in literature on afterpulses which occurred in the 52-58.5 ns and 190-198 ns ranges after the main pulse. These pulses appeared at a higher rate. They were consistently present in all three 8854's. The afterpulses in the 52-58.5 ns range were generated by He^+ ions, in existence between the second and third dynode, striking the second dynode and causing the secondary emission. The afterpulses in the 190-198 ns range were caused by He^+ ions between the first and the second dynode, causing the secondary emission from the first dynode.

Afterpulse time spectra measurements were made on ITT 4129f using the microchannel plate voltage of 2500 V. The photomultiplier gain was 1.6×10^6. This new generation device has a 7 nm thick ion barrier film between the photocathode and the input face of the first microchannel plate to prevent the bombardment of the photocathode by positive ions. Introduction of the film has resulted in a significant improvement in the photocathode quantum efficiency stability and life expectancy. Furthermore, extensive studies of the performance characteristics of this device have shown that the introduction of the film has resulted in total elimination of the afterpulses. Similarly, no afterpulses were detected in the Hamamatsu R1564U microchannel plate photomultipliers with protective film. In this device the entrance part of the first microchannel plate is covered with a thin aluminum film. In contrast, all microchannel plate photomultipliers without protective film made by various manufacturers have demonstrated the strong afterpulsing phenomena and the photocathode quantum efficiency decrease during operating time.[7,8,11,18]

Afterpulses were detected in the 50 ns, 200 ns, 250 ns and 320 ns time regions. They were identified on the basis of the ion mass-to-charge ratio with the following species: H_2^+, H_2O^+, $N_2^+ + CO^+$ and CO_2^+. Furthermore, it was also shown that the afterpulse appearance probability increases proportionally with the number of photoelectrons in the pulse and the device gain. The appearance probability has shown a strong dependence on the residual gas pressure inside the vacuum envelope and the outgassing status of the microchannel plate.[11] The only disadvantage of the usage of the thin protective film between the photocathode and the input face microchannel plate is a reduction of photoelectron collection efficiency of the device input electron optics. According to preliminary calculations the collection efficiency can be reduced by approx. 20-30% depending on the particular photomultiplier and its operating conditions.

At present, physical processes responsible for the existance of the afterpulses in the 8.5-14 μs time range are not well understood. The very late appearance of afterpulses after the main output pulse eliminates a possibility of the optical feedback from the electroluminescence of the dynodes to the photocathode and the afterpulses generation at the photocathode or dynodes by positive ions. This conclusion is based on calculations of electron and positive ion transit times between the photocathode, the first, second and third dynode and the photomultiplier anode, taking into account the electric field distribution and the mass-to-charge ratio of various single ions and ionized molecules as well as the device geometry. The very late afterpulses appearing in the 5 μs and 40 μs time range after the main pulse were also reported in Ref. 23 in more recently manufactured 8850's. However, they were not observed in the same photomultipliers produced 10 years ago.[15] More experimental work is required before the nature of these sometimes observed, very late afterpulses can be determined.

In addition to the He^+ ions which are mainly responsible for the afterpulses, the H^+ and H_2^+ ions were also identified in some conventionally designed and microchannel plate photomultipliers[10,11,13] which were manufactured at a particular time. However, there is disagreement in literature concerning the afterpulses generated by oxygen positive ions. Results reported in Ref. 9 strongly suggest that no afterpulses are produced by oxygen. This conclusion is based on an experiment where small quantities of various gasses were introduced into the demountable photomultiplier to determine unambiguously the associated afterpulses. In this experiment afterpulses were produced and identified with various introduced gasses (Xe^+, A^+, N_2^+ and H_2^+) but not with oxygen. This result is in contrast with experimental data reported in Ref. 10 where presumably the O^+ ion afterpulses were observed in the 747-900 ns time range for the sealed 8852 photomultiplier. Later, results were reported in Ref. 13 which indicated difficulties to localize the time position of O^+ and O^{2+} afterpulses as well as to obtain agreement between theoretical considerations and experimental data. In our measurements,[12,15] we have not detected af-

terpulses which can be identified with oxygen ions. In general, the possibility of detecting the oxygen related afterpulses is extremely small because the oxygen molecules inside the photomultiplier envelope are immediately absorbed by the alkali metals of the photocathode or possible getter material. Consequently, afterpulses previously assigned to oxygen ions may be due to other gaseous species such as OH.

The experimental evidence mentioned above and in cited references clearly shows that photomultipliers have a long usable lifetime without serious increases in afterpulses in a typical laboratory environment. Necessary corrections should be made, however, in single photon counting systems to account for the existence of afterpulses when accurate results from the fluorescence lifetime measurements are required. This is particularly important in experimental situations where lifetime measurements are made over a dynamic range of several decades. Under some experimental conditions where ambient concentration of helium is artificially elevated by the emission from helium Dewar bottles or gas Cherenkov counters, the probability of generating afterpulses increases significantly.[19] In this case, the photocathode quantum efficiency decreases in a relatively short time period because the photocathode is continuously bombarded by highly concentrated helium positive ions. The effect of afterpulses can be reduced by introducing a dead time in the measuring system. In such cases, the deadtime should be adjusted to a value which will not compromise the system measuring accuracy.[24]

Table 1. Afterpulse Performance of 8850 and 8854 Photomultipliers

		8850 Photomultiplier			8854 Photomultiplier		
Afterpulse Count Rate (cps)	Measurement Time Interval	0-680ns	450ns-7μs	4.5μs-68μs	0-680ns	450ns-7μs	4.5μs-68μs
	Single Photoelectron Pulse Rate = 100kHz	171 at 18ns 155 at 351ns 310 at 415ns	b	b	106 at 58.5ns 5.5 at 190ns	b	b
	Single Photoelectron Pulse Rate = 10kHz	b	a	b	b	0.8 at 933ns	b
	Single Photoelectron Pulse Rate = 1kHz	b		a	b		a
	Three Photoelectron Pulse Rate = 10kHz	5.8 at 19ns 181 at 350ns 362 at 413ns	a	a	10.4 at 59ns 12 at 198ns	2 at 956ns	9 at 9.2μs 14 at 14μs

a - Afterpulses were not observed.

b - Measurement was not made due to a measuring system limitation.

ACKNOWLEDGMENTS

This work was performed as part of the program of the Electronics Research and Development Group of the Department of Instrument Science and Engineering of Lawrence Berkeley Laboratory, and was partially supported by the U.S. Department of Energy under Contract No. DE-AC03-76SF00098. The author would like to express his appreciation to Dr. George Morton for his clarifying comments.

Reference to a company or product name does not imply approval or recommendation of the product by the University of California or the U. S. Department of Energy to the exclusion of others that may be suitable.

REFERENCES

(1) B. LESKOVAR, C.C. LO, P.R. HARTING, K.H. SAUER: Rev. Sci. Instr. 47, 1113 (1976)
(2) P.R. HARTING, K.H. SAUER, C.C. LO, B. LESKOVAR: Rev. Sci. Instr. 47, 1122 (1976)
(3) B. LESKOVAR: IEEE Trans. Nucl. Sci. NS-32, 1232 (1985)
(4) B. LESKOVAR: Proc. of the 1980 Deep Underwater Muon and Neutrino Detection Signal Processing Workshop, A. Roberts, Ed., 21 (U. of Hawaii, Honolulu, 1980)
(5) A.G. WRIGHT: Ibid, 45
(6) C. CORY, D. SMITH, C. WUEST, J.G. LEARNED, H.A.W. TOTHILL, J. WARDLEY, A.G. WRIGHT: IEEE Trans. Nucl. Sci. NS-28, 445 (1981)
(7) L.P. HOCKER, P.A. ZAGARINO, J. MADRID, D. SIMONS, B. DARIS, P.B. LYONS: IEEE Trans. Nucl. Sci. NS-26, 356 (1979)
(8) P.R. LYONS, L.D. LOONEY, J. OGLE, R.D. SIMMONS, R. SELK, B. HOPKINS, L. HOCKER, M. NELSON, P. ZAGARINO: Los Alamos Scientific Lab. Report No. LA-UR-81-1028 (1981)
(9) G.A. MORTON, H.M. SMITH, R. WASSERMAN: IEEE Trans. Nucl. Sci. NS-14, 443 (1967)
(10) P.B. COATES: J. Phys. D: Appl. Phys. 6, 1159 (1973)
(11) K. OBA, P. REHAK: IEEE Trans. Nucl. Sci. NS-28, 683 (1981)
(12) C.C. LO, B. LESKOVAR: IEEE Trans. Nucl. Sci. NS-29, 184 (1982)
(13) S. TORRE, T. ANTONIOLI, P. BENETTI: Rev. Sci. Instr. 54, 1777 (1983)
(14) A.G. WRIGHT: J. Phys. E: Sci. Instr. 16, 300 (1983)
(15) C.C. LO, B. LESKOVAR: IEEE Trans. Nucl. Sci. NS-30, 445 (1983)
(16) C.C. LO, B. LESKOVAR: IEEE Trans. Nucl. Sci. NS-31, 413 (1984)
(17) C.C. LO, B. LESKOVAR: IEEE Trans. Nucl. Sci. NS-32, 360 (1985)
(18) W.C. PASKE: Rev. Sci. Instr. 45, 1001 (1974)
(19) D.F. BARLLETT, A.L. DUNCAN, J.R. ELLIOTT: Rev. Sci. Instr. 52, 265 (1981)
(20) B. LESKOVAR, C.C. LO: IEEE Trans. Nucl. Sci. NS-19, 58 (1972)
(21) B. LESKOVAR: Proc. of the 5th International Congress, Laser 81-Optoelectronics 381 (Munich, West Germany, 1982)
(22) B. LESKOVAR: Proc. of the 6th International Congress, Laser 83-Optoelectronics 68 (Munich, West Germany, 1984)
(23) M. YAMASHITA, S. TAKEUCHI: IEEE Trans. Nucl. Sci. NS-31, 438 (1984)
(24) B.H. CANDY: Rev. Sci. Instr. 56, 183 (1985)

TECHNICAL INFORMATION DEPARTMENT
LAWRENCE BERKELEY LABORATORY
UNIVERSITY OF CALIFORNIA
BERKELEY, CALIFORNIA 94720